The Stellar Content of Local Group Galaxies
IAU Symposium, Vol. 192, 1999
Patricia Whitelock and Russell Cannon, eds.

The Distance and Orientation of the Galactic Bulge from Mira Variables: A Preliminary Report

R.M. Catchpole

Royal Observatory Greenwich, Greenwich, London SE10 9NF, UK
Institute of Astronomy, Madingley Road, Cambridge, CB3 OHA, UK

P.A. Whitelock

S A Astronomical Observatory, PO Box 9, Observatory, 7935, S Africa

M.W. Feast

University of Cape Town, Private Bag, Rondebosch, 7700, S Africa

S.M.G. Hughes

Institute of Astronomy, Madingley Road, Cambridge, CB3 OHA, UK

C. Alard

Observatoire de Paris, 61 Ave. de l'Observatoire, F-75014, Paris

E. Olivier

University of Western Cape, Private Bag X17, Bellville, 7535, S Africa
S A Astronomical Observatory, PO Box 9, Observatory, 7935, S Africa

Abstract. Near-infrared, *JHKL*, observations of 595 Mira variables in two fields on either side of the centre of our Galaxy, confirm that the Bulge is not spherically symmetric about its axis of rotation, but is elongated so that the part to the east of the centre is closer to us. The shape of the Bulge about its axis of rotation is not uniquely defined by these data, but the shape that deviates least from circular symmetry has an axis ratio $x_o/y_o = 1.7$, with a major axis at an angle, $\theta = 58° \pm 7$, to the plane of the sky, for a galactic centre distance, $R_0 = 9.4 \pm 0.5$ kpc. This is based on an assumed scale length in galactic coordinates of $b_o = 375$ pc and $l_o/b_o = 2.0$.

1. Introduction

Whitelock & Catchpole (1992), using IRAS selected Mira variables, showed that the Bulge has a bar-like structure inclined so that stars at positive longitude (East) are closer than those at negative longitude (West). This has also been seen in the COBE data, e.g. by Binney et al. (1997).

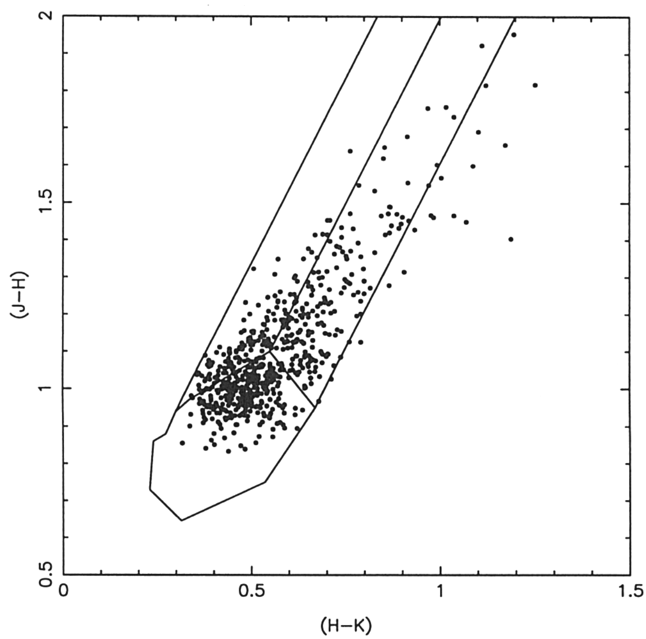

Figure 1. Two-colour plot for the Miras showing the Mira box and its reddened extension.

In the Large Magellanic Cloud, Miras show a tight relationship between period and absolute K (2.2μm) magnitude, M_K. This property and their intrinsic brightness at K, as well as the fact that the effects of interstellar extinction are greatly reduced at K, makes them ideal probes of the structure of our Bulge.

We selected two fields, both at $b = -7°$, centred at $l = +8°$ (Bulge East) and $l = -8°$ (Bulge West) and each covering about 25 square degrees. The UK Schmidt Telescope of the AAO was used to obtain about 15 IV-N (I-band) plates in each field, over an interval of 6 years. Data were also obtained for two other fields centred at $l = 3°, b = -4°$ (Bulge Centre) and $l = 2°$ and $b = -15°$ (Bulge South).

2. Data reduction

The Schmidt plates were scanned, using both APM in Cambridge and MAMA at the Paris Observatory, to find the long period variable candidates and their periods. The candidates were then observed with the SAAO 1.9m telescope to obtain $JHKL$ photometry. Few stars have so far more than two measurements. A $(J - H)$, $(H - K)$ two-colour diagram, Fig. 1, is used to identify the Mira variables. The region for unreddened local Miras is defined in this diagram and all stars lying outside this region and its reddened extension, were eliminated. This leaves a total of 341 stars in Bulge West, 254 in Bulge East and 43 stars in Bulge Centre and Bulge South. Hereafter we will call these Miras, and Fig. 2 shows them in a period–colour plot.

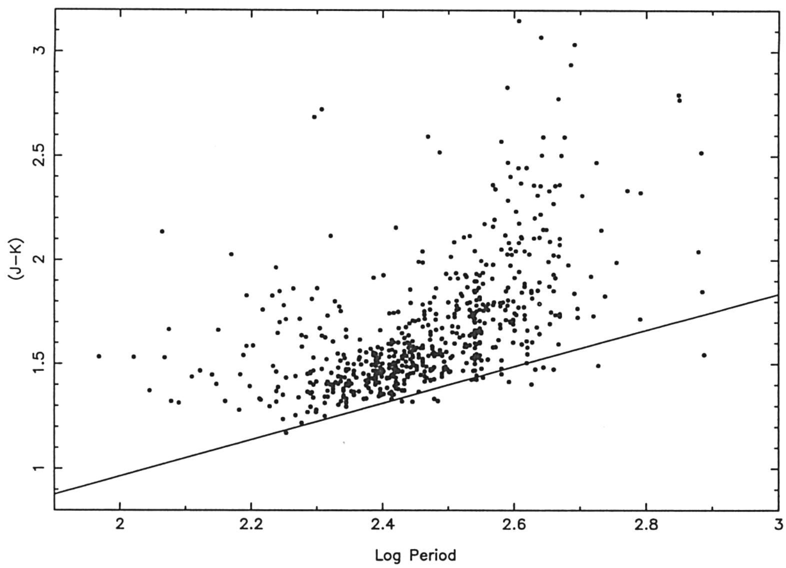

Figure 2. Period–colour relation for the Miras. The line is the locus for local Miras.

The Miras were then de-reddened using the relationship adopted by Whitelock et al. (1999 in preparation) for local Miras:

$$(J-K)_0 = 0.872\log P - 0.779.$$

Distance moduli were found for each star using the slope of the $K, \log P$ relation for the LMC found by Feast et al. (1989), with a zero point of 0.84 mag found by Whitelock et al., using Hipparcos observations of 185 local Miras:

$$M_K = -3.47\log P + 0.84.$$

3. Bulge Model

In order to interpret the resulting distribution of Mira distance moduli, we model the Bulge with a triaxial ellipsoidal stellar distribution, where the number of stars, N, per unit volume, can be expressed as:

$$N \propto e^{-(x^2/x_o^2+y^2/y_o^2+z^2/z_o^2)^{1/2}}.$$

Here x, y, and z are distances from the Centre of the Galaxy along the three axes of the ellipsoid with scale lengths x_o, y_o, and z_o. The x axis is tilted at some angle θ to the plane of the sky and lies in the plane of the Galaxy for which $b = 0°$. The z axis is perpendicular to the plane of the Galaxy. The axes and sign conventions are shown in Fig. 3.

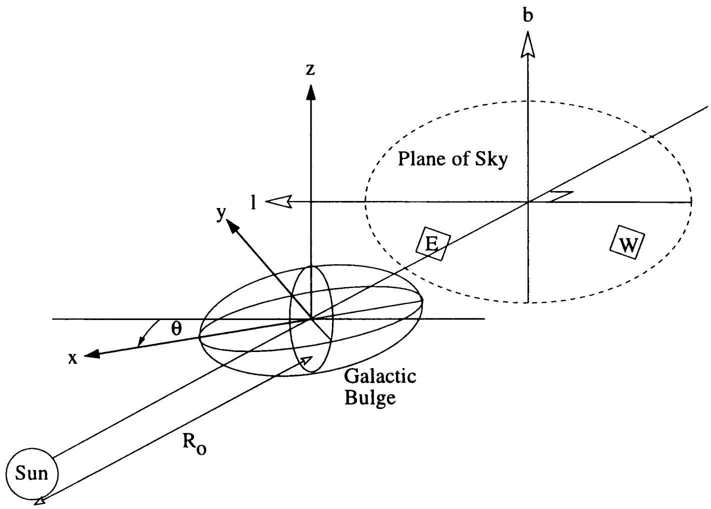

Figure 3. Sign and axis convention and location of the E and W fields.

4. Results

The COBE data show that in the infrared the Galactic Bulge has an ellipsoidal shape with a ratio of $l_o/b_o \simeq 2$ and a scale height of 2.37°, corresponding to $b_o = 370$ pc for $R_0 = 9$ kpc. Wyse et al. (1997) suggest that to a first order the Bulge has a scale height of about 350 pc; Binney et al. (1997) have built a more complex model of the bulge with $x_o/z_o \simeq 2.5$, $x_o/y_o \simeq 1.67$, $x_o \simeq 1900$ pc and $\theta = 70°$.

In order to find the best values of R_0 and θ from our data, we adopt $l_o/b_o = 2$ and construct models with various values of l_o and x_o/y_o for a range of values of θ. For each set of models, x_o and x_o/z_o are varied as a function of θ so that l_o and l_o/b_o, the projection of the model on the plane of the sky, remains constant. However, the projection of the model onto the plane of the sky does not give a perfect exponential distribution in surface density. The values of l_o and l_o/b_o are found by least squares fitting the projected model along the l and b directions between 2° and 12°.

For a given set of input parameters, x_o, x_o/y_o, x_o/z_o, θ and an initial value of R_0, the model is used to determine the mean modulus along lines of sight corresponding to the l & b of each star. The difference between the observed and predicted modulus for each star is formed and these differences are then summed over all the stars for which the difference in modulus is $< \pm 1.6$ mag and the mean difference is used to predict a new value of R_0. This process is converged to find a final value of R_0. The standard deviation of the observed moduli is also found. This is done separately for the East and West fields. The resulting values of R_0 are then plotted as a function of θ and the intercepts of the curves for Bulge East and West give the appropriate values of R_0 and θ. For $x_o/y_o \leq 1.67$ there are no intercepts while for $x_o/y_o \geq 1.7$ there are generally two intercepts giving two values of R_0 and θ. The resulting values of R_0 and θ are listed in Tables 1 & 2. The models are all for $l_o/b_o = 2.0$, a

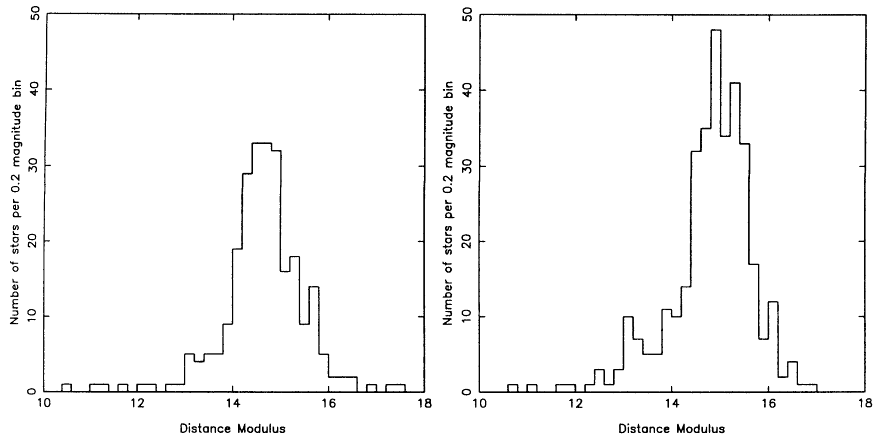

Figure 4. The Distance Modulus distribution for Bulge East on the left and Bulge West on the right.

range of x_o/y_o and for $l_o \simeq 500$ pc in Table 1 and $l_o \simeq 1000$ pc in Table 2. The internal errors on the values of R_0 and θ in Tables 1 & 2, based on the observed dispersion in the modulus, are $\Delta R_0 = \pm 0.3$ kpc and $\Delta\theta = \pm 5°$. The column marked RMS gives the average taken over the East and West fields, of the root-mean-square of the residuals for the model modulus distribution. The observed RMS of the distance modulus distribution for the two fields is 0.61 mag (see Fig. 4). The wide variation in the model RMS should help eliminate some of the models when an accurate budget of the observed RMS can be made. This must allow for incomplete light curve coverage, dispersion in the $K, \log P$ relation and uncertainty in the reddening corrections.

Table 1. Bulge Parameters for $l_o/b_o = 2.0$ and $l_o \simeq 500$ pc

x_o/y_o	x_o (pc)	x_o/z_o	l_o (pc)	R_0 (kpc)	θ^o	RMS
1.7	589	2.67	507	9.6	63	0.21
1.7	493	2.45	457	9.5	55	0.18
2.0	757	3.65	509	10.5	76	0.29
2.0	471	2.10	500	9.2	37	0.12
4.0	440	1.96	495	9.0	26	0.06

Table 2. Bulge Parameters for $l_o/b_o = 2.0$ and $l_o \simeq 1000$ pc

x_o/y_o	x_o (pc)	x_o/z_o	l_o (pc)	R_0 (kpc)	θ^o	RMS
1.7	1170	2.69	1017	9.2	64	0.31
1.7	989	2.35	1001	9.2	50	0.24
2.0	1449	3.42	984	9.5	74	0.39
2.0	877	2.15	987	9.1	36	0.17
4.0	2500	7.50	873	12.1	81	0.56
4.0	820	2.02	981	9.0	26	0.08

5. Discussion

As noted above the data indicate a lower limit to the ellipticity of the Bulge about its axis of rotation. At this limit the solution for R_0 and θ are single valued. $x_o/y_o = 1.7$ is sufficiently close to this limit that it is appropriate to average the values of R_0 and θ for this ratio. Interestingly this solution gives a shape and orientation for the Bulge similar to that found by Binney et al. (1997) from their de-projection of the COBE surface photometry.

In future it may be possible to eliminate the $x_o/y_o = 4.0$ model used by Whitelock & Catchpole (1992) by deducing the intrinsic dispersion in the observed modulus distribution and comparing it with the very small RMS predicted by the model for the large and small value of θ respectively. In fact the $x_o/y_o = 4.0$, $\theta = 81°$ model can already be eliminated because the dispersion for the West field is equal to that of the data, allowing no room for intrinsic scatter in the data.

Although the value of θ remains uncertain and depends on the model of the Bulge, the distance to the centre, R_0, is less dependent and lies between $9.0 \leq R_0 \leq 10.5$ kpc.

Taking the average distances and scale heights for the $x_o/y_o = 1.7$ model for both the $l_o \simeq 500$ pc and the $l_o \simeq 1000$ pc case leads to the following result: $R_0 = 9.4 \pm 0.5$ kpc, for $l_o = 745$ pc, $b_o = 372$ pc and $l_o/b_o = 2.0$. This distance is very close to the value of $R_0 = 9.3 \pm 0.7$ kpc given by Reid (1998). Reid's distance is ultimately based on a determination of the distance to M5 by fitting its main sequence with local sub-dwarfs using Hipparcos parallax observations. It is interesting to note the agreement in the distance to the Galactic Centre based on the distance calibration of local Miras used here and that based on the sub-dwarf calibration of the distance to M5, both ultimately depend on Hipparcos observations.

The greatest remaining systematic uncertainty in the distance to the centre, based on Mira observations, lies in possible systematic differences in their properties at the Galactic Centre and in the solar neighbourhood. However, the similarity of the period-colour relations in the Bulge and in the solar neighbourhood may suggest that any systematic differences between the Miras in these environments are small.

References

Binney, J., Gerhard, O., Spergel, D. 1997, MNRAS, 288, 365

Feast, M.W., Glass, I.S., Whitelock, P.A., Catchpole, R.M. 1989, MNRAS, 241, 375

Reid, I.N. 1998, AJ, 115, 204

Whitelock, P.A., Catchpole, R.M. 1992, in: *The Center, Bulge and Disk of the Milky Way*, (ed.) L. Blitz, Kluwer Academic Publishers, p. 103

Wyse, R.F.G., Gilmore, G., Franx, M. 1997, ARA&A, 35, 637